SDHC Promoter Methylation, a Novel Pathogenic Mechanism in Parasympathetic Paragangliomas

Cristóbal Bernardo-Castiñeira,[1] Nuria Valdés,[2] Marta I. Sierra,[3] Inés Sáenz-de-Santa-María,[1] Gustavo F. Bayón,[3] Raúl F Perez,[3,4] Agustín F. Fernández,[3] Mario F. Fraga,[4] Aurora Astudillo,[5] Rafael Menéndez,[6] Belén Fernández,[7] Maribel del Olmo,[8] Carlos Suarez,[1] and María-Dolores Chiara[1]

[1]Head and Neck Oncology Laboratory, Institute of Sanitary Research of Asturias (ISPA), Hospital Universitario Central de Asturias, Institute of Oncology of Asturias (IUOPA), CIBERONC, 33011 Oviedo, Spain; [2]Service of Endocrinology and Nutrition, Hospital Universitario Central de Asturias, Oviedo, Spain; [3]Cancer Epigenetics Laboratory, Institute of Oncology of Asturias (IUOPA), Institute of Sanitary Research of Asturias (IISPA), Hospital Universitario Central de Asturias, Universidad de Oviedo, Oviedo, Spain; [4]Nanomaterials and Nanotechnology Research Center (CINN-CSIC), Universidad de Oviedo–Principado de Asturias, Spain; [5]Service of Pathology, Hospital Universitario Central de Asturias, Oviedo, Spain; [6]Service of Radiology, Hospital Universitario Central de Asturias, Oviedo, Spain; [7]Service of Nuclear Medicine, Hospital Universitario Central de Asturias, Oviedo, Spain; and [8]Service of Endocrinology and Nutrition, Hospital Universitario la Fé, Valencia, Spain

Context: Germline mutations in the succinate dehydrogenase A, B, C, and D genes (collectively, *SDHx*) predispose to the development of paragangliomas (PGLs) arising at the parasympathetic or sympathetic neuroendocrine systems. *SDHx* mutations cause absence of tumoral immunostaining for SDHB. However, negative SDHB immunostaining has also been found in a subset of PGLs that lack *SDHx* mutations.

Settings: Here, we report the comprehensive molecular characterization of one such a tumor of parasympathetic origin compared with healthy paraganglia and other PGLs with or without *SDHx* mutations.

Results: Integration of multiplatform data revealed somatic *SDHC* methylation and loss of the 1q23.3 region containing the *SDHC* gene. This correlated with decreased *SDHC* messenger RNA (mRNA) and protein levels. Furthermore, another genetic event found affected the *VHL* gene, which showed a decreased DNA copy number, associated with low *VHL* mRNA levels, and an absence of VHL protein detected by immunohistochemistry. In addition, the tumor displayed a pseudohypoxic phenotype consisting in overexpression of the hypoxia-inducible factor 1α (HIF-1α) and miR-210, as well as downregulation of the iron-sulfur cluster assembly enzyme (ISCU) involved in SDHB maturation. This profile resembles that of *SDHx*- or *VHL*-mutated PGLs but not of PGLs with decreased *VHL* copy number, pointing to *SDHC* rather than *VHL* as the pathogenic driver.

Conclusions: Collectively, these findings demonstrate the potential importance of both the *SDHC* epigenomic event and the activation of the HIF-1α/miR-210/ISCU axis in the pathogenesis of *SDHx* wild-type/SDHB-negative PGLs. Moreover, this is the first case of a sporadic parasympathetic PGL that carries silencing of *SDHC*, fulfilling the two-hit Knudson's model for tumorigenesis. **(*J Clin Endocrinol Metab* 103: 1–11, 2018)**

ISSN Print 0021-972X ISSN Online 1945-7197
Printed in USA

Received 31 July 2017. Accepted 31 October 2017.
First Published Online ■■■ ■■■ 2017

Abbreviations: CGH, comparative genomic hybridization; CNV, copy number variant; GIST, gastrointestinal stromal tumor; HIF, hypoxia-inducible factor; ISCU, iron-sulfur cluster assembly enzyme; MLPA, multiplex ligation-dependent probe amplification; mRNA, messenger RNA; PCC, pheochromocytoma; PCR, polymerase chain reaction; PGL, paraganglioma; TSS, transcription start site.

Paragangliomas (PGLs) and pheochromocytomas (PCCs) are rare neuroendocrine tumors of the parasympathetic and sympathetic nervous system (1). Parasympathetic PGLs typically develop in the head and neck region, whereas sympathetic PGLs are frequently located at the abdomen or thorax. PCCs are a special type of PGLs derived from the chromaffin cells at the adrenal medulla. Parasympathetic PGLs are typically treated surgically, the first-line therapeutic choice, or by radiotherapy. Unfortunately, the complexity of the anatomy of the skull base and the proximity of tumors to main arteries and nerves lead, inevitably, to a high rate of severe iatrogenic morbidity even through the use of safe embolization protocols and sophisticated surgical approaches. The limited knowledge of the molecular basis of these tumors has precluded the development of effective drug-based therapies.

Although the molecular mechanisms involved in tumor development are not completely understood, the fact that ~40% of tumors are hereditary has shed some light on the pathogenesis of this disease. Mutations in *SDHB*, *SDHC*, *SDHA*, and *SDHD* genes increase the risk of developing hereditary PCC/PGLs (2). These genes (collectively *SDHx* genes) encode the four core subunits of the mitochondrial succinate dehydrogenase (SDH) complex, which links the Krebs cycle and the oxidative phosphorylation pathway. In addition, mutations in the *SDHAF2* gene, encoding an auxiliary subunit required for SDH function, have also been associated with hereditary PGLs/PCCs (3). Other PGL/PCC susceptibility genes include *RET*, *VHL*, *NF1*, *TMEM127*, *MAX*, *KIF1B*, and *EGLN1* (4, 5). Mutations in any of these genes could lead to the development of sympathetic PGLs/PCCs, whereas parasympathetic PGLs are more specifically linked to mutations in the *SDHx* genes (6). Aside from the hereditary component, less is known about the genetic drivers of the "sporadic" PGLs/PCCs developing in the absence of known hereditary pathogenic mutations. Nevertheless, multiplatform molecular characterization studies have revealed that sporadic PCCs/PGLs may also be driven by somatic alterations affecting the same PGL/PCC-susceptibility genes (4, 6–8).

Mutations in the *SDHx* genes abolish SDH's ability to convert succinate to fumarate, leading to succinate accumulation in the cell. It has been hypothesized that succinate accumulation leads to activation of the hypoxia-inducible factor (HIF) (9–11), known to be involved in abnormal cell growth and tumor formation (12). Regarding activation of HIF, recent reports showed either moderated or strong activation of HIF-related pathways in PGLs/PCCs associated with *SDHx* or *VHL* mutations, respectively (13–16). Among the different targets of the HIF transcription factor, the microRNA, miR-210, is thought to play a major role in PGLs/PCCs because of its induced downregulation of the Fe-S cluster assembly enzyme, iron-sulfur cluster assembly enzyme (ISCU), which is required for maturation of mitochondrial proteins containing Fe-S clusters such as SDHB (14).

Recent reports have shown that the *SDHx*-mutated PGLs/PCCs can be easily identified in surgical tumor specimens by immunohistochemistry. Specifically, *SDHx*-mutated tumors show absence of SDHB protein detected by immunohistochemistry (17–19), and *SDHA*-mutated tumors also have loss of SDHA immunostaining (20). Although the mechanism involved in loss of SDHB is not fully understood, it is plausible that *SDHx* mutations lead to decreased preassembly of the SDHC-SDHD or SDHA-SDHB complexes at the inner mitochondrial membrane and that this interferes with maturation of the heterotetrameric protein complex, leading to destabilization of the SDHB protein. On the other hand, upon mitochondrial import, SDHA and SDHB proteins mature by flavination of SDHA by SDHAF2 and the insertion of three Fe-S clusters generated by ISCU. Thus, modification of the protein levels or molecular structure of SDHAF2 or ISCU may also alter SDH complex stability (15). In this same line, some *SDHB* mutations cause impaired Fe-S cluster incorporation into SDHB, thus rendering the protein unstable (21).

Recent reports highlighted the existence of a small subset of PGLs/PCCs that lack SDHB protein but do not harbor *SDHx* mutations, suggesting that mechanisms independent of *SDHx* mutations may be involved in SDHB protein silencing (6, 17, 22). In this report, we have explored the molecular mechanism involved in SDHB silencing of a parasympathetic PGL that lacked mutations in *SDHx* genes. In addition, we have compared the data in that tumor to those of healthy paraganglia and other PGLs with or without *SDHx* mutations. The putative involvement of the HIF-1α/miR-210/ISCU pathway was also analyzed in the tumor under analysis. We describe the first published case of a parasympathetic PGL harboring *SDHC* methylation likely involved in tumorigenesis.

Materials and Methods

Experimental design

Our previous work showed an absence of SDHB immunostaining in some PGLs lacking *SDHx* and *VHL* mutations (14). This was striking and suggestive of pathogenic mechanisms alternative to *SDHx* mutations impinging on SDH activity. This study was aimed at deciphering molecular mechanisms involved in silencing of SDHB protein in one of these tumors, hereafter designated as PGLmx. Exome sequencing, array–comparative

genomic hybridization (array-CGH) targeting tumor suppressor genes, genome-wide methylation analysis, quantitative reverse transcription polymerase chain reaction (PCR), and immunohistochemistry studies were performed in PGLmx. Data were compared with those of healthy paraganglia (carotid body) and other PGLs lacking or not the *SDHx* mutation (clinical and genetic features are described in Supplemental Table S2).

The selected case was a jugular PGL developed in a man at age 29 years. This patient lacked a family history of PCCs/PGLs. The tumor had been surgically treated and incompletely removed. Five years later, magnetic resonance imaging showed a rounded lump that included the mastoids and partially covered the internal carotid artery compatible with tumor recurrence. At the retroperitoneal space, two lesions with diameters ~10 and 11 mm each were identified with moderated contrast uptake (Fig. 1). These lesions were compatible with PGLs. Scintigraphy and Tc99m-Tektrotyd photon emission computed tomography studies revealed pathological uptake in the mastoid region but not in the retroperitoneal space. Diagnosis was recurrence of jugular PGL and two putative nonfunctional retroperitoneal PGLs. The patient was asymptomatic and the therapeutic strategy was wait-and-see. Two years later, in October 2017, he remained asymptomatic.

Tumor specimens

Tumor and blood samples were obtained from patients with PGLs or PCCs, diagnosed and treated between 2005 and 2016 in the Hospital Universitario Central de Asturias. For DNA-based studies, fragments were obtained from the core of the tumor and contained >60% tumor cells. Tumor specimens were snap-frozen at the time of surgical resection and stored at −80°C in RNAlater (Ambion) until processed. Informed consent was obtained from the patients, and the study was approved by the ethical committee of our institution.

Mutation analysis

Genomic DNA was isolated using the QIAmp DNA Mini kit (Qiagen, Inc., Chatsworth, CA) and subsequently treated with RNase A (1 U/mL) at 37°C for 5 minutes. Mutation analysis of *SDHA*, *SDHB*, *SDHC*, *SDHD*, and *VHL* genes was performed by direct sequencing as previously described. *SDHx* and *VHL* genes were analyzed for the presence of large deletions in tumor DNA using the multiplex ligation-dependent probe amplification (MLPA) method as recommended by the manufacturer (MRC Holland, The Netherlands).

Array-CGH

Screening of genome-wide copy number variants (CNVs) was carried out by array-CGH using the OncoNIM Familial Cancer platform, a 60K Agilent-based custom array-CGH (Nimgenetics, Madrid, Spain). This custom array covers the whole genome with a median spatial resolution of 1 probe per 150 kb, with high-density coverage in 20 genes related to familial cancer (100-bp median spatial resolutions for these genes). Hybridizations were performed according to the manufacturer's protocols. A commercially available male DNA sample (Promega, Madison, WI) was used as reference DNA. Microarray data were extracted and visualized using the Feature Extraction Software v10.7 and Agilent Genomic Workbench v.5.0 (Agilent Technologies, Santa Clara, CA) using ADAM-2 (windown 0.5 Mb, A = 10) as an aberration detection statistic. Genomic build NCBI37 (Hg19) was used for delineating the genomic coordinates of the detected CNVs.

Q:7

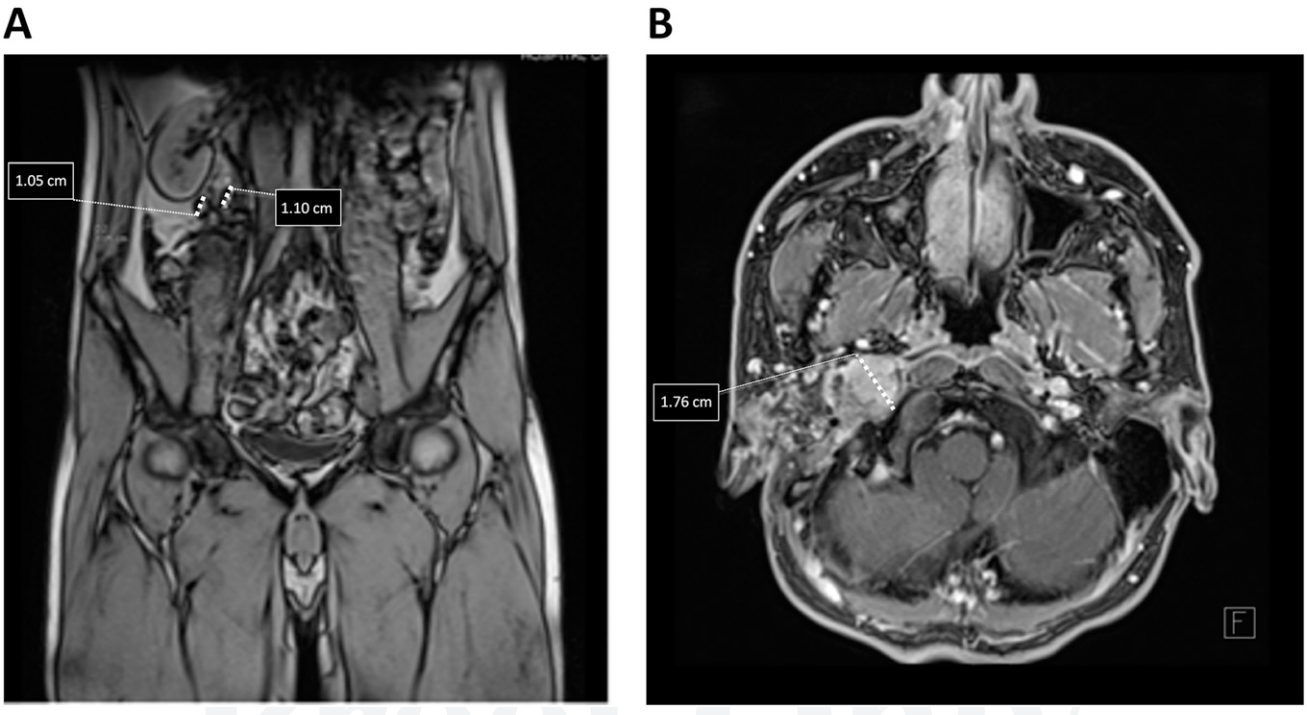

Figure 1. Magnetic resonance imaging studies in PGLmx. Magnetic resonance images of the (A) coronal and (B) axial planes of the abdomen and skull base, respectively, of PGLmx showing one lesion in the mastoid region and two in the retroperitoneal space. Diameters of those lesions are shown in centimeters.

Exome sequencing

Genomic DNA (3 μg) was sheared and used for the construction of a paired-end sequencing library as described in the protocol provided by Illumina (San Diego, CA). Enrichment of exonic sequences was then performed for each library using the SureSelect Human All Exon 50-Mb kit (Agilent) following the manufacturer's instructions. Exon-enriched DNA was precipitated with magnetic beads coated with streptavidin (Invitrogen), washed, and eluted. An additional 18 cycles of amplification were then performed on the captured library. Exon enrichment was validated by real-time PCR in a 7300 Real-Time PCR System (Applied Biosystems) using a set of two pairs of primers to amplify exons and one pair to amplify an intron. Enriched libraries were sequenced in one lane of the Illumina Gene Analyzer II× sequencer, using the standard protocol. Read mapping and data processing were done by DreamGenics S.L. (http://www.dreamgenics.com/dreamgenics). Mean and median coverage were >40 for all *SDHx* genes and *SDHAF2* and *VHL*.

Genome-wide methylation analysis

DNA was extracted with phenol/chloroform/isoamyl alcohol and bisulfite converted before genome-wide analysis of methylation with the Infinium Human Methylation450 BeadChip array (Illumina) in the Spanish "Centro Nacional de Genotipado" CEGEN-ISCIII. Raw data files were imported and preprocessed using R/Bioconductor package minfi (version 1.14.0) (23). Methylation raw signals were normalized using the SWAN method (24). A methylation measure was defined to be defective if it had a detection *P* value >0.01. Probes with >2 defective measures and samples with >5000 defective measures were removed from the data set. Methylation was described as a β value, which ranges between 0 (no methylation) and 1 (full methylation). The β values of probes located 2000 bp upstream and 200 bp downstream the transcription start site (defined as promoter regions) of the parasympathetic PGL-susceptibility genes (*SDHA*, *SDHB*, *SDHC*, *SDHD*, *SDHAF2*, and *VHL*) were extracted and analyzed in comparison with healthy carotid bodies. The methylation level of selected CpGs was validated by pyrosequencing (PyromarkQ24 Advanced System). Primers used for PCR amplification and sequencing were designed with the PyroMark assay designer (Supplemental Table S3). The genomic region included in the analysis has been previously reported (25, 26). The statistical significance of the differences between groups of tumors was assessed using a *t* test with a significance threshold of 0.05.

Immunohistochemistry

SDHB, SDHC, SDHA, VHL, and HIF-1α expression was evaluated by immunohistochemistry in tissue sections from the surgically resected PGLs as previously described (14). Following published recommendations (27), both the percentage of immunostained cells and the intensity of staining were used to quantify HIF-1α protein expression. SDHC antibody (Abcam) showed granular cytoplasmic staining similar to that obtained with SDHA or SDHB antibodies, as previously reported (28). Data were reviewed independently by three investigators.

MicroRNA/messenger RNA quantification

Total RNA was isolated with the *mir*Vana miRNA Isolation Kit (Ambion) according to the manufacturer's instructions. TaqMan assay (Applied Biosystems) was used to analyze the expression of the mature human miR-210. For microRNA quantification, 10 ng total RNA was used in the RT reaction, and the transcribed complementary DNA was then used for subsequent PCR amplification using the TaqMan 2X Universal PCR Master Mix, No AmpErase UNG (Applied Biosystems) as described by the manufacturer. RNU44 expression was assayed for normalization. For *SDHx* and *VHL* messenger RNA (mRNA) quantification, PCR reactions were performed by using the SYBR Green PCR Master Mix (Applied Biosystems) and the thermocycler conditions recommended by the manufacturer. Each sample was analyzed for cyclophilin A mRNA to normalize for RNA input amounts and to perform relative quantification. All reactions were performed in triplicate, and relative microRNA/mRNA expression was normalized against endogenous controls using the comparative $\Delta\Delta$ CT method.

Statistical analysis

All statistical analyses were performed using SPSS statistical software version 19 (SPSS, Inc., Chicago, IL) as previously described. $P < 0.05$ was defined as statistically significant.

Results

Genetic alterations

An initial search for germline mutations of the most frequently mutated genes in parasympathetic PGLs, *SDHB*, *SDHC*, and *SDHD*, by Sanger sequencing, revealed an absence of mutations in PGLmx. MLPA analysis of the *SDHx* genes also revealed an absence of genetic losses at the germline level. Subsequent exome sequencing of the tumoral genomic DNA ruled out the presence of somatic mutations in any of the known PCC/PGL-susceptibility genes. It also confirmed that the tumor was not inherited by germline mutations in *SDHx* genes or in any of the other PCC/PGL-susceptibility genes.

Array-CGH in tumor DNA, targeting 30 tumor suppressor genes (Supplemental Table S1), showed partial deletions at chromosome 1 containing locus 1p36.13 and 1q23.3 where *SDHB* and *SDHC* are localized, respectively (Fig. 2A). Other genetic loss affected *VHL* at chromosome 3 (Fig. 2B) but not other PCC/PGL-susceptibility genes such as *SDHD*, *SDHAF2*, *MEN1*, and *FH* (data not shown). Genetic loss of *VHL* was verified by MLPA assay in tumor DNA (Fig. 2C). In contrast, this assay revealed an absence of *VHL* deletion in germinal DNA. Estimation of somatic copy number alterations, based on exome sequencing data (29), confirmed deletions of chromosome regions containing *SDHC* and *VHL* genes (Fig. 2D and 2E) but not of *SDHB*. Besides *SDHC*, genomic regions containing *NDUFS2*, *FCER1G*, *AL590714.1*, *APOA2*, *TOMM40L*, *MIR5187*, *NR1I3*, *PCP4L1*, and *MPZ* at 1p36.13 also showed decreased copy number. None of these genes have been linked to PGL or PCC development.

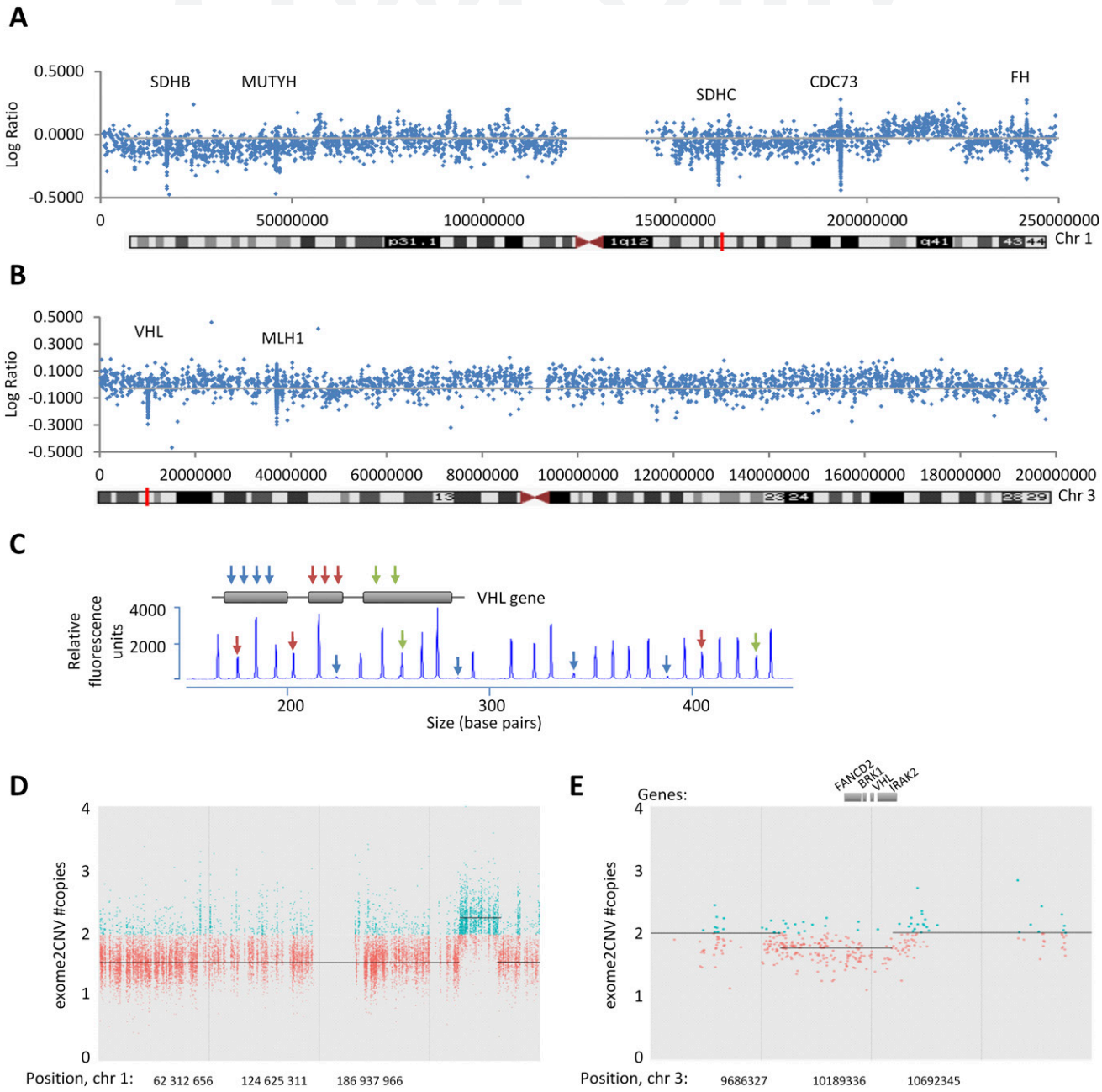

Figure 2. Heterozygous loss of *SDHC* and *VHL* genes in PGLmx tumor. (A, B) Array-CGH screening of genomic DNA in PGLmx. Profiles are displayed as normalized log2 signal intensity ratios of each spot on the array to the genomic position at (A) chromosome 1 and (B) chromosome 3. Genes with high density of probes in the array are indicated. *VHL* points to the chr3:10182692-10193904 (Human GRCh37/hg19) genomic region. (C) Upper panel shows a schematic representation of the structure of the *VHL* gene; arrows indicate location of the probes included in the MLPA. Capillary gel electrophoresis images depicting the MLPA assay for *VHL* in tumor DNA. (D, E) Normalized exome coverage data are determined for each individual capturing exon in the PGLmx tumor sample and blood sample from the same patient. The tumor/normal ratio is calculated for each probe. Copy number alterations in PGLmx are indicated by dark gray lines. DNA copies below or above two are indicated by red or blue dots, respectively.

Epigenetic alterations

DNA methylation arrays of the tumor genomic DNA were performed and compared with that of three samples of human healthy carotid bodies and 17 PCCs/PGLs. Promoter regions of *SDHB*, *SDHD*, *SDHA*, *SDHAF2*, or *VHL* were not found differentially methylated either in PGLmx or in the other PGLs included in the array. In contrast, the data showed high methylation percentages in the promoter of *SDHC* in PGLmx (Fig. 3A). This epigenetic alteration was not identified in two tumors lacking *SDHx* mutations and carrying somatic deletion of *VHL* exon 1 (14). Methylation status of *SDHC* gene around the transcription start site (TSS) in PGLmx was verified by pyrosequencing (Fig. 3B). Pyrosequencing of

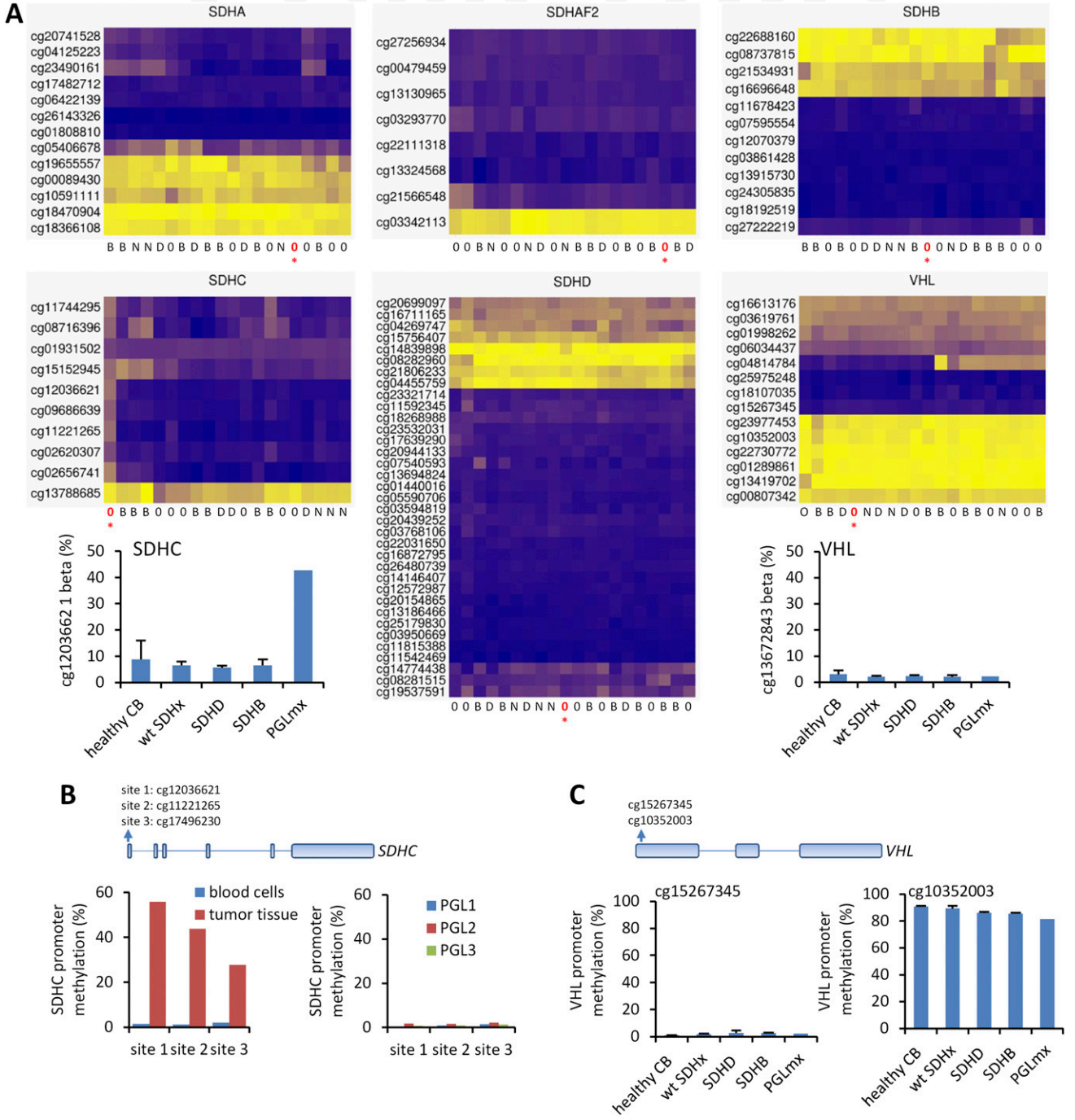

Figure 3. *SDHC* TSS methylation in PGLmx. (A) Unsupervised hierarchical cluster analysis of normalized methylation β values of healthy carotid bodies (N) and parasympathetic PGLs carrying *SDHB* (B), *SDHD* (D), or no *SDHx* mutations (0). PGLmx sample is indicated by red 0*. Quantification (mean ± standard deviation value) of the β values corresponding to the cg12036621 (*SDHC* TSS) and cg13672843 (*VHL* promoter) probes in the indicated group of tumors is shown below the *SDHC* and *VHL* data heatmap, respectively. (B, C) Schematic representations of the (B) *SDHC* and (C) *VHL* genes indicating the location of the CpG sites identified by the indicated probes and selected for validation. *SDHC* TSS methylation percentages for the indicated genomic sites were determined by directed pyrosequencing in (B, left panel) tumor and blood samples from PGLmx and (B, right panel) three other parasympathetic PGLs (PGLs 1 to 3) harboring SDHB-positive immunostaining in the absence of *SDHx* mutations. *VHL* promoter methylation percentages (mean ± standard deviation value) for the indicated genomic regions determined by pyrosequencing in tumor samples from one healthy carotid body (CB); five, four, and two PGLs without *SDHx* mutations [wild-type (wt) *SDHx*]; or with *SDHD* or *SDHB* mutations, respectively.

VHL CpG sites also confirmed the absence of differential methylation in PGLmx compared with healthy carotid body or other PGLs lacking *SDHx* alterations (n = 6 tumors) (Fig. 3C).

We tested blood from a patient with PGLmx for *SDHC* TSS methylation and found no *SDHC* methylation (Fig. 3A), consistent with postzygotic onset of *SDHC* methylation rather than germline inheritance. This

suggests a process of *SDHC* reprogramming during tumor development.

Absence of SDHC methylation in other SDHB-negative/SDHx wild-type PGLs

Our previous study had identified three other parasympathetic PGLs with loss of SDHB protein in the absence of *SDHx* mutations (14). Therefore, we analyzed whether those tumors also harbored somatic *SDHC* TSS methylation. This analysis showed low methylation levels in the three tumors that were similar to those of normal carotid bodies (Fig. 3B). Thus, *SDHC* methylation does not seem to be a frequent event in SDHB-negative/*SDHx* wild-type parasympathetic PGLs.

SDHx and VHL gene expression

To determine whether gene alterations of *SDHC*, *SDHB*, and/or *VHL* result in deregulations at the mRNA level, quantitative reverse transcription PCR analysis of *SDHC*, *SDHB*, and *VHL* genes was performed in tumor complementary DNA, in a healthy carotid body, and in eight parasympathetic PGL samples [five wt*SDHx* (tumors lacking *SDHx* mutations) and three mut*SDHx* (tumors with *SDHB* or *SDHD* mutations)]. As shown in Fig. 4A, decreased *SDHC* mRNA levels were found in the PGLmx tumor compared with wt*SDHx* tumors or the normal carotid body, although levels were similar to that of mut*SDHB* or mut*SDHD* tumors. In contrast, *SDHB*, *SDHA*, *SDHD*, and *SDHAF1* mRNA levels were Q:11 significantly higher (threefold) in the PGLmx tumor than in the other PGLs (Fig. 4B).

For the analysis of *VHL* mRNA levels, we included two types of parasympathetic PGLs as controls: tumors with wild-type *VHL* (wt *VHL*) and tumors carrying deletions of exon 1 of *VHL* (del-*VHL*), which are known to express low levels of *VHL* mRNA (14). As shown in Fig. 4C, *VHL* mRNA levels of PGLmx were significantly lower than those of wt *VHL*-PGLs and similar to those of del-*VHL* tumors.

SDHB, *SDHA*, and *SDHC* expression was also analyzed at the protein level (Fig. 5). This confirmed the absence of immunostaining for SDHB and strong SDHA immunolabeling, as shown in our previous reports, and revealed decreased SDHC expression compared with other parasympathetic PGLs (a representative image of a SDHB-mutant PGL is shown in Fig. 5D), which is consistent with the absence of *SDHA* mutation, epigenetic silencing of *SDHC*, and decreased *SDHC* CNV. VHL immunohistochemistry was also shown to be negative (Fig. 5).

HIF-1α/miR-210/ISCU signaling pathway

The analysis of the HIF-1α/miR-210/ISCU axis in the PGLmx tumor revealed high expression levels of HIF-1α (immunoscore: 75, Fig. 5), which was above the median value detected in parasympathetic PGLs (median value: 33) (14). This study also showed increased levels of miR-210 and lower levels of *ISCU* mRNA compared with normal paraganglia (Fig. 6).

Discussion

Complete loss of SDHB protein expression, as determined by immunohistochemistry, is a common feature of *SDHx*-mutated tumors. However, recent reports have alerted about the existence of SDHB loss in the absence of *SDHx* mutations (17–19). The molecular scrutiny of one Q:12 such tumor, described here, has revealed the presence of two major genetic alterations consisting of (1) the somatic epigenetic silencing and loss of heterozygosis of the *SDHC* gene, accompanied by low *SDHC* expression at the mRNA and protein levels, and (2), decreased copy number of the *VHL* gene, low *VHL* mRNA levels, and absence of VHL protein in the tumor.

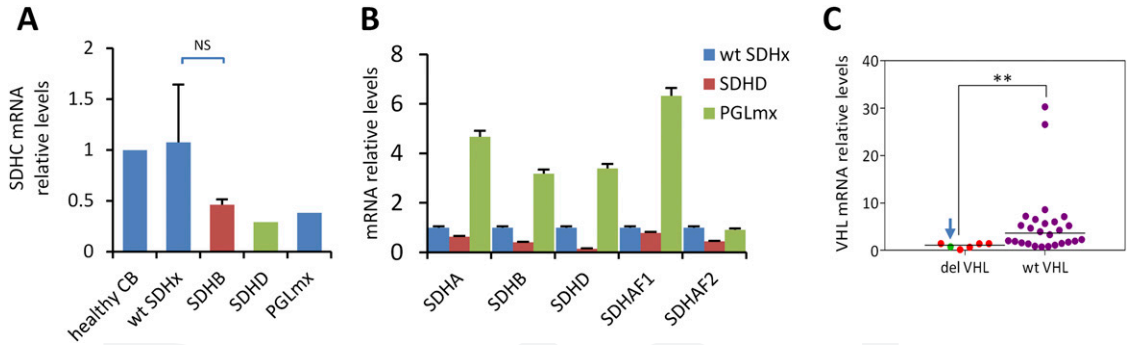

Figure 4. Decreased *VHL* and *SDHC* mRNA levels in PGLmx. (A, B) mRNA relative levels (mean ± standard deviation value) of (A) *SDHC* and (B) *SDHA*, *SDHB*, *SDHD*, *SDHAF1*, and *SDHAF2* in one healthy carotid body (CB), PGLs lacking *SDHx* mutations [wild-type (wt) *SDHx*; n = 5], PGLs harboring *SDHB* (n = 2) or *SDHD* (n = 1) mutations, and PGLmx. (C) mRNA relative levels of *VHL* in PGLs lacking *SDHx* mutations and harboring (del *VHL*) or not (wt *VHL*) exon 1 deletion of *VHL*. Blue arrow and green dot denotes *VHL* mRNA levels in PGLmx. NS indicates not significant; $^{**}P < 0.005$.

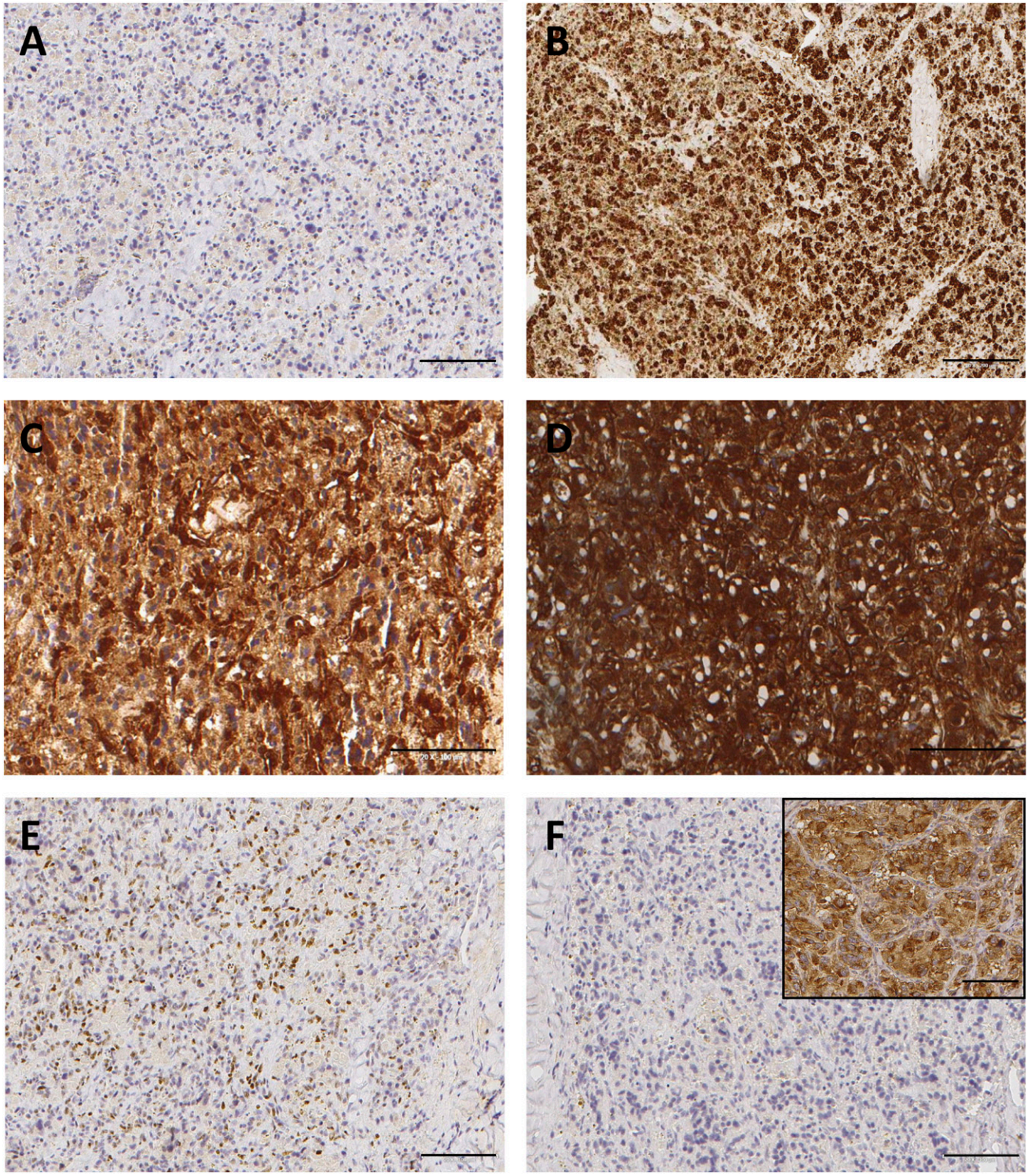

Figure 5. SDHB, SDHA, SDHC, HIF-1α, and VHL immunostainings in PGLmx. Representative images of (A) SDHB, (B) SDHA, (C, D) SDHC, (E) HIF-1α, and (F) VHL immunostainings in (A–C, E–F) PGLmx and (D) a PGL with SDHB mutation. Inset in panel F shows a representative image of VHL immunostaining of a *SDHx* wild-type PGL. Asterisks denote stained blood vessels. Scale bars = 100 μm.

Recent reports described for the first time that *SDHC* methylation could be involved in tumorigenesis (25, 26, 28, 30). In line with the case described here, all those tumors shared a similar phenotype: deficiency of SDH activity in the absence of *SDHx* mutations. The first works reported that gastrointestinal stromal tumors (GISTs) that developed in patients with (9 patients) or without (14 patients) the Carney triad are caused by hypermethylation of the *SDHC* promoter (25, 26, 30). Two of the patients with the Carney triad also developed

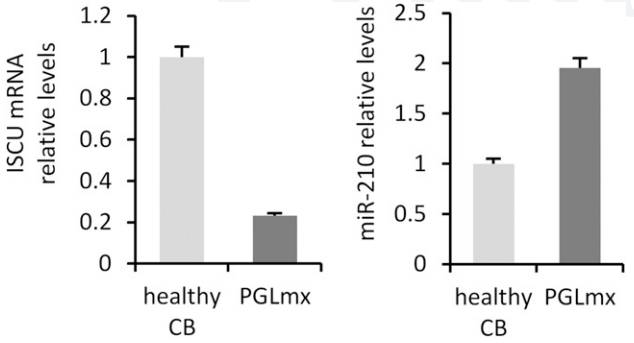

Figure 6. ISCU and miR-210 RNA levels in PGLmx. miR-210 and ISCU mRNA levels were analyzed in PGLmx and compared with those of a human normal carotid body (CB).

sympathetic PGLs, which carried *SDHC* hypermethylation (26). Compound heterozygosity (monoallelic methylation and mutation of *SDHC*) or homozygous *SDHC* methylation was found in 4 and 12 GISTs, respectively (26). *SDHC* loss of heterozygosis has not been reported for the remaining cases (25, 26, 30). *SDHC* epigenetic alteration was more recently found in two sympathetic PGLs that developed in one patient, apparently out of the context of the Carney triad (28). Similarly to some GISTs, loss of heterozygosis was not identified in those two PGLs. However, the fact that epigenetic modification of the *SDHC* gene was the only event identified in those patients suggested that this genetic alteration was a plausible mechanism of functional impairment of the SDH complex and tumorigenesis.

The case reported here has similarities but also some differences with those GIST and PGL cases previously reported. The tumor displays loss of SDHB protein, absence of *SDHx* mutations, and *SDHC* TSS methylation, which was consistent with the low levels of *SDHC* mRNA and of the SDHC protein detected by immunostaining. We also found that the epigenetic modification of *SDHC* was accompanied by the heterozygous loss of the chromosomal region containing the *SDHC* gene, consistent with the Knudson two-hit model for tumorigenesis. Recent clinical review (7 years after diagnosis of the jugular paraganglioma) revealed the absence of other tumors related to the Carney triad or Carney-Stratakis syndrome such as GISTs or pulmonary chondroma. Thus, this case adds to the previously reported PGL case not associated with Carney syndrome and represents the first case involving *SDHC* TSS methylation and loss of heterozygosis in a parasympathetic PGL. However, even though the *SDHC* genetic events fulfill the two-hit model to attribute it a pathogenic role, the unambiguous claiming of its involvement in PGL tumorigenesis is not a straightforward conclusion. This is because, in contrast to the other reported cases, we found that the PGLmx tumor harbored an additional genetic defect concerning another PGL-related gene. This consisted of decreased *VHL* gene dosage and mRNA levels, as well as absence of VHL protein detected by immunohistochemistry. These types of *VHL* deregulations have been previously reported in a subtype of parasympathetic PGLs, the so-called del-*VHL*-PGLs (14). A previous report also described the coexistence of alterations in two susceptibility genes (somatic deletion of the *VHL* gene and somatic *SDHC* mutation) in sporadic PCCs (31). The functional significance of partial loss of *VHL* is, thus far, unknown. Indeed, del-*VHL*-PGLs do not display the distinctive pseudohypoxic phenotype of *VHL*- or *SDHx*-related tumors as, for example, the strong or moderated activation of the HIF-1α/miR-210/ISCU pathway found in *VHL*-mutated or *SDHx*-mutated PGLs, respectively (14). Furthermore, del-*VHL*-PGLs do not harbor the low levels of SDHB protein typically found in *VHL*-mutated PGLs (15). Importantly, in contrast to del-*VHL*-PGLs, the case described here harbors activation of the HIF-1α/miR-210/ISCU pathway and lacks SDHB protein, thus resembling *SDHx*-mutated rather than del-*VHL*-PGLs. These features tip the balance toward a pathogenic role of *SDHC* rather than *VHL*, although they do not allow definitely ruling out a not yet identified role of VHL protein. In any case, irrespective of whether it is *VHL*, *SDHC*, or both, the drivers of the activation of the HIF pathway, the fact is that the PGLmx tumor displays reduced levels of ISCU protein, which is known to participate in the maturation of SDHB by the insertion of three Fe-S clusters (32). Thus, it is tempting to speculate that loss of SDHB protein was due to an additive effect of loss of both *SDHC* and *ISCU*.

Although the mechanism involved in aberrant *SDHC* hypermethylation is unknown, a causative role of *VHL* deletion does not seem likely given that our study included two "sporadic" parasympathetic PGLs that carry a decreased *VHL* DNA copy number and decreased *VHL* mRNA levels (as PGLmx) but lack *SDHC* hypermethylation. Somatic mosaicism has been proposed as a mechanism for *SDHC* hypermethylation in patients with GIST given that low-levels *SDHC* hypermethylation had been found in blood and saliva of patients (26). In contrast to those studies, *SDHC* hypermethylation was not identified in the blood DNA of the patient analyzed in the present work. Nevertheless, a role of tissue-specific mosaicism epigenetically affecting the *SHC* gene cannot be ruled out. Further work on other tissues could shed some light into this relevant issue.

Taken together, the identification of the *SDHC* TSS methylation and heterozygous loss of *SDHC* gene fulfills the two-hit Knudson model for cancer initiation, providing an explanation for the tumorigenesis of sporadic parasympathetic PGLs lacking SDHB protein expression.

Furthermore, we also provide data suggesting the activation of the HIF-1α/miR-210/ISCU axis, which could be also involved in tumorigenesis of the *SDHC*-epimutated PGLs. Importantly, this type of tumors could be identified in surgical specimens by SDHB and SDHC immunohistochemistry, which should be negative or weak positive for both. This is of clinical relevance given that a histopathological analysis could allow the identification of patients carrying *SDHC* methylation. Finally, our data raise the possibility that patients with *SDHC*-epimutated PGLs could benefit from hypomethylating drugs and/or agents targeting HIF. Further research on a wide series of PGLs with negative SDHB immunostaining and absence of *SDHx* mutations is indicated to get to know the real extent of this type of genetic alterations in sporadic tumors.

Acknowledgments

We thank Eva Allonca for technical assistance and Xose S. Puente for critical reading of the manuscript and comments on exome sequencing data.

Financial Support: This work was supported by Instituto de Salud Carlos III–Fondo de Investigación Sanitaria (FIS PI11/929), Fundación para el Fomento en Asturias de la Investigación Científica Aplicada y la Tecnología (GRUPIN14-003), and Q:14 European Regional Development funds (FEDER, CIBERONC).

Correspondence and Reprint Requests: María-Dolores Q:15 Chiara, Head and Neck Oncology Laboratory, Institute of Sanitary Research of Asturias (ISPA), Hospital Universitario Central de Asturias, Avda de Roma s/n, 33011 Oviedo, Spain. Q:16 E-mail: mdchiara.uo@uniovi.es.

Disclosure Summary: The authors have nothing to disclose.

References

1. Fishbein L. Pheochromocytoma and paraganglioma: genetics, diagnosis, and treatment. *Hematol Oncol Clin North Am*. 2016;**30**(1):135–150.
2. Benn DE, Robinson BG, Clifton-Bligh RJ. 15 Years of paraganglioma: clinical manifestations of paraganglioma syndromes types 1–5. *Endocr Relat Cancer*. 2015;**22**(4):T91–T103.
3. Bayley J-P, Kunst HP, Cascon A, Sampietro ML, Gaal J, Korpershoek E, Hinojar-Gutierrez A, Timmers HJ, Hoefsloot LH, Hermsen MA, Suárez C, Hussain AK, Vriends AH, Hes FJ, Jansen JC, Tops CM, Corssmit EP, de Knijff P, Lenders JW, Cremers CW, Devilee P, Dinjens WN, de Krijger RR, Robledo M. SDHAF2 mutations in familial and sporadic paraganglioma and phaeochromocytoma. *Lancet Oncol*. 2010;**11**(4):366–372.
4. Fishbein L, Leshchiner I, Walter V, Danilova L, Robertson AG, Johnson AR, Lichtenberg TM, Murray BA, Ghayee HK, Else T, Ling S, Jefferys SR, de Cubas AA, Wenz B, Korpershoek E, Amelio AL, Makowski L, Rathmell WK, Gimenez-Roqueplo AP, Giordano TJ, Asa SL, Tischler AS, Pacak K, Nathanson KL, Wilkerson MD; Cancer Genome Atlas Research Network. Comprehensive molecular characterization of pheochromocytoma and paraganglioma. *Cancer Cell*. 2017;**31**(2):181–193.
5. Buffet A, Venisse A, Nau V, Roncellin I, Boccio V, Le Pottier N, Boussion M, Travers C, Simian C, Burnichon N, Abermil N, Favier J, Jeunemaitre X, Gimenez-Roqueplo A-PA. A decade (2001–2010) of genetic testing for pheochromocytoma and paraganglioma. *Horm Metab Res*. 2012;**44**(5):359–366.
6. Currás-Freixes M, Inglada-Pérez L, Mancikova V, Montero-Conde C, Letón R, Comino-Méndez I, Apellániz-Ruiz M, Sánchez-Barroso L, Aguirre Sánchez-Covisa M, Alcázar V, Aller J, Álvarez-Escolá C, Andía-Melero VM, Azriel-Mira S, Calatayud-Gutiérrez M, Díaz JÁ, Díez-Hernández A, Lamas-Oliveira C, Marazuela M, Matias-Guiu X, Meoro-Avilés A, Patiño-García A, Pedrinaci S, Riesco-Eizaguirre G, Sábado-Álvarez C, Sáez-Villaverde R, Sainz de Los Terreros A, Sanz Guadarrama Ó, Sastre-Marcos J, Scolá-Yurrita B, Segura-Huerta Á, Serrano-Corredor ML, Villar-Vicente MR, Rodríguez-Antona C, Korpershoek E, Cascón A, Robledo M. Recommendations for somatic and germline genetic testing of single pheochromocytoma and paraganglioma based on findings from a series of 329 patients. *J Med Genet*. 2015;**52**(10):647–656.
7. Luchetti A, Walsh D, Rodger F, Clark G, Martin T, Irving R, Sanna M, Yao M, Robledo M, Neumann HPH, Woodward ER, Latif F, Abbs S, Martin H, Maher ER. Profiling of somatic mutations in phaeochromocytoma and paraganglioma by targeted next generation sequencing analysis. *Int J Endocrinol*. 2015;**2015**:1–8.
8. Stenman A, Welander J, Gustavsson I, Brunaud L, Bäckdahl M, Söderkvist P, Gimm O, Juhlin CC, Larsson C. *HRAS* mutation prevalence and associated expression patterns in pheochromocytoma. *Genes Chromosomes Cancer*. 2016;**55**(5):452–459.
9. Hewitson KS, Liénard BMR, McDonough MA, Clifton IJ, Butler D, Soares AS, Oldham NJ, McNeill LA, Schofield CJ. Structural and mechanistic studies on the inhibition of the hypoxia-inducible transcription factor hydroxylases by tricarboxylic acid cycle intermediates. *J Biol Chem*. 2006;**282**(5):3293–3301.
10. Koivunen P, Hirsilä M, Remes AM, Hassinen IE, Kivirikko KI, Myllyharju J. Inhibition of hypoxia-inducible factor (HIF) hydroxylases by citric acid cycle intermediates: possible links between cell metabolism and stabilization of HIF. *J Biol Chem*. 2006;**282**(7):4524–4532.
11. Tannahill GM, Curtis AM, Adamik J, Palsson-McDermott EM, McGettrick AF, Goel G, Frezza C, Bernard NJ, Kelly B, Foley NH, Zheng L, Gardet A, Tong Z, Jany SS, Corr SC, Haneklaus M, Caffrey BE, Pierce K, Walmsley S, Beasley FC, Cummins E, Nizet V, Whyte M, Taylor CT, Lin H, Masters SL, Gottlieb E, Kelly VP, Clish C, Auron PE, Xavier RJ, O'Neill LAJ. Succinate is an inflammatory signal that induces IL-1β through HIF-1α. *Nature*. 2013;**496**(7444):238–242.
12. Semenza GL. Hypoxia-inducible factors: mediators of cancer progression and targets for cancer therapy. *Trends Pharmacol Sci*. 2012;**33**(4):207–214.
13. de Cubas AA, Leandro-García LJ, Schiavi F, Mancikova V, Comino-Méndez I, Inglada-Pérez L, Perez-Martinez M, Ibarz N, Ximénez-Embún P, López-Jiménez E, Maliszewska A, Letón R, Gómez Graña A, Bernal C, Alvarez-Escolá C, Rodríguez-Antona C, Opocher G, Muñoz J, Megias D, Cascón A, Robledo M. Integrative analysis of miRNA and mRNA expression profiles in pheochromocytoma and paraganglioma identifies genotype-specific markers and potentially regulated pathways. *Endocr Relat Cancer*. 2013;**20**(4):477–493.
14. Merlo A, Bernardo-Castiñeira C, Sáenz-de-Santa-María I, Pitiot AS, Balbín M, Astudillo A, Valdés N, Scola B, Del Toro R, Méndez-Ferrer S, Piruat JI, Suarez C, Chiara M-D. Role of VHL, HIF1A and SDH on the expression of miR-210: implications for tumoral pseudo-hypoxic fate. *Oncotarget*. 2017;**8**(4):6700–6717.
15. Merlo A, de Quiros SB, Secades P, Zambrano I, Balbín M, Astudillo A, Scola B, Arístegui M, Suarez C, Chiara M-D. Identification of a signaling axis HIF-1α/microRNA-210/ISCU independent of SDH mutation that defines a subgroup of head and neck paragangliomas. *J Clin Endocrinol Metab*. 2012;**97**(11):E2194–E2200.

16. Merlo A, de Quirós SB, de Santa-María IS, Pitiot AS, Balbín M, Astudillo A, Scola B, Arístegui M, Quer M, Suarez C, Chiara M-D. Identification of somatic VHL gene mutations in sporadic head and neck paragangliomas in association with activation of the HIF-1α/miR-210 signaling pathway. *J Clin Endocrinol Metab*. 2013; **98**(10):E1661–E1666.
17. Papathomas TG, Oudijk L, Persu A, Gill AJ, van Nederveen F, Tischler AS, Tissier F, Volante M, Matias-Guiu X, Smid M, Favier J, Rapizzi E, Libe R, Currás-Freixes M, Aydin S, Huynh T, Lichtenauer U, van Berkel A, Canu L, Domingues R, Clifton-Bligh RJ, Bialas M, Vikkula M, Baretton G, Papotti M, Nesi G, Badoual C, Pacak K, Eisenhofer G, Timmers HJ, Beuschlein F, Bertherat J, Mannelli M, Robledo M, Gimenez-Roqueplo AP, Dinjens WN, Korpershoek E, de Krijger RR. SDHB/SDHA immunohistochemistry in pheochromocytomas and paragangliomas: a multicenter interobserver variation analysis using virtual microscopy: a Multinational Study of the European Network for the Study of Adrenal Tumors (ENS@T). *Mod Pathol*. 2015;**28**(6):807–821.
18. Gill AJ, Benn DE, Chou A, Clarkson A, Muljono A, Meyer-Rochow GY, Richardson AL, Sidhu SB, Robinson BG, Clifton-Bligh RJ. Immunohistochemistry for SDHB triages genetic testing of SDHB, SDHC, and SDHD in paraganglioma-pheochromocytoma syndromes. *Hum Pathol*. 2010;**41**(6):805–814.
19. van Nederveen FH, Gaal J, Favier J, Korpershoek E, Oldenburg RA, de Bruyn EM, Sleddens HF, Derkx P, Rivière J, Dannenberg H, Petri BJ, Komminoth P, Pacak K, Hop WC, Pollard PJ, Mannelli M, Bayley JP, Perren A, Niemann S, Verhofstad AA, de Bruïne AP, Maher ER, Tissier F, Méatchi T, Badoual C, Bertherat J, Amar L, Alataki D, Van Marck E, Ferrau F, François J, de Herder WW, Peeters MP, van Linge A, Lenders JW, Gimenez-Roqueplo AP, de Krijger RR, Dinjens WN. An immunohistochemical procedure to detect patients with paraganglioma and phaeochromocytoma with germline SDHB, SDHC, or SDHD gene mutations: a retrospective and prospective analysis. *Lancet Oncol*. 2009;**10**(8):764–771.
20. Korpershoek E, Favier J, Gaal J, Burnichon N, van Gessel B, Oudijk L, Badoual C, Gadessaud N, Venisse A, Bayley J-P, van Dooren MF, de Herder WW, Tissier F, Plouin P-F, van Nederveen FH, Dinjens WNM, Gimenez-Roqueplo A-P, de Krijger RR. SDHA immunohistochemistry detects germline *SDHA* gene mutations in apparently sporadic paragangliomas and pheochromocytomas. *J Clin Endocrinol Metab*. 2011;**96**(9):E1472–E1476.
21. Saxena N, Maio N, Crooks DR, Ricketts CJ, Yang Y, Wei M-H, Fan TW-M, Lane AN, Sourbier C, Singh A, Killian JK, Meltzer PS, Vocke CD, Rouault TA, Linehan WM. SDHB-deficient cancers: the role of mutations that impair iron sulfur cluster delivery. *J Natl Cancer Inst*. 2015;**108**(1):djv287.
22. Castelblanco E, Santacana M, Valls J, de Cubas A, Cascón A, Robledo M, Matias-Guiu X. Usefulness of negative and weak-diffuse pattern of SDHB immunostaining in assessment of SDH mutations in paragangliomas and pheochromocytomas. *Endocr Pathol*. 2013;**24**(4):199–205.
23. Aryee MJ, Jaffe AE, Corrada-Bravo H, Ladd-Acosta C, Feinberg AP, Hansen KD, Irizarry RA. Minfi: a flexible and comprehensive Bioconductor package for the analysis of Infinium DNA methylation microarrays. *Bioinformatics*. 2014;**30**(10):1363–1369.
24. Maksimovic J, Gordon L, Oshlack A. SWAN: subset-quantile within array normalization for illumina infinium HumanMethylation450 BeadChips. *Genome Biol*. 2012;**13**(6):R44.
25. Haller F, Moskalev EA, Faucz FR, Barthelmeß S, Wiemann S, Bieg M, Assie G, Bertherat J, Schaefer I-M, Otto C, Rattenberry E, Maher ER, Ströbel P, Werner M, Carney JA, Hartmann A, Stratakis CA, Agaimy A. Aberrant DNA hypermethylation of SDHC: a novel mechanism of tumor development in Carney triad. *Endocr Relat Cancer*. 2014;**21**(4):567–577.
26. Killian JK, Miettinen M, Walker RL, Wang Y, Zhu YJ, Waterfall JJ, Noyes N, Retnakumar P, Yang Z, Smith WI, Killian MS, Lau CC, Pineda M, Walling J, Stevenson H, Smith C, Wang Z, Lasota J, Kim SY, Boikos SA, Helman LJ, Meltzer PS. Recurrent epimutation of SDHC in gastrointestinal stromal tumors. *Sci Transl Med*. 2014; **6**(268):268ra177.
27. Gong L, Zhang W, Zhou J, Lu J, Xiong H, Shi X, Chen J. Prognostic value of HIFs expression in head and neck cancer: a systematic review. *PLoS One*. 2013;**8**(9):e75094.
28. Richter S, Klink B, Nacke B, de Cubas AA, Mangelis A, Rapizzi E, Meinhardt M, Skondra C, Mannelli M, Robledo M, Menschikowski M, Eisenhofer G. Epigenetic mutation of the succinate dehydrogenase C promoter in a patient with two paragangliomas. *J Clin Endocrinol Metab*. 2016;**101**(2):359–363.
29. Valdés-Mas R, Bea S, Puente DA, López-Otín C, Puente XS. Estimation of copy number alterations from exome sequencing data. *PLoS One*. 2012;**7**(12):e51422.
30. Urbini M, Astolfi A, Indio V, Heinrich MC, Corless CL, Nannini M, Ravegnini G, Biasco G, Pantaleo MA. SDHC methylation in gastrointestinal stromal tumors (GIST): a case report. *BMC Med Genet*. 2015;**16**(1):87.
31. Weber A, Hoffmann MM, Neumann HPH, Erlic Z. Somatic mutation analysis of the SDHB, SDHC, SDHD, and RET genes in the clinical assessment of sporadic and hereditary pheochromocytoma. *Horm Cancer*. 2012;**3**(4):187–192.
32. Rouault TA, Tong WH. Iron-sulfur cluster biogenesis and human disease. *Trends Genet*. 2008;**24**(8):398–407.

Proof Only

AUTHOR QUERIES

AUTHOR PLEASE ANSWER ALL QUERIES

Q: 1_Please provide postal codes for affiliations 2 to 8.

Q: 2_Please confirm that given names and surnames are identified properly by the colors indicated. Colors will not appear in print or online, and are for proofing and coding purposes only to ensure proper indexing on PubMed.

Q: 3_Please verify all author names and affiliations.

Q: 4_Please confirm the city for affiliation 4.

Q: 5_Any alternations between capitalization and/or italics in genetic terminology have been retained per the original manuscript. Please confirm that all genetic terms have been formatted properly throughout. (Note that the standard convention is to represent genes in italic font and proteins in roman font.)

Q: 6_Priority claims ("novel," "first") need a qualifying phrase such as "to our knowledge," per journal style. Please supply a similar type of phrase for the sentence that begins "Moreover, this is the first case …" and each "novel" mention in the article.

Q: 7_Some but not all manufacturer locations were provided in your original manuscript. To ensure consistency, please provide the location (city and state/country) for all manufacturers that currently do not cite a location.

Q: 8_Please define "CEGEN-ISCIII."

Q: 9_Please define "SWAN."

Q: 10_Please define "RT."

Q: 11_Per journal style, "significant" and "significantly" should be used only for statistics (e.g., "statistically significant effect"). Please confirm whether "significantly" should be changed to "statistically significant" or whether another term, such as "substantial," should be used here and throughout.

Q: 12_Reference 30 has been deleted because it is a duplicate of reference 19. The rest of the citations and references have been renumbered accordingly. Please confirm the changes.

Q: 13_Should "Carney syndrome" be "Carney-Stratakis syndrome" in the sentence that begins "Thus, this case adds.…"?

Q: 14_Please confirm that the financial support statement is correct and complete as set.

Q: 15_Please provide degree for corresponding author (MD, PhD, etc.).

Q: 16_Please verify the corresponding author's contact information.